Supplementary Information

The RSC chromatin remodeling enzyme plays a unique role in directing the accurate positioning of promoter nucleosomes

Wippo CJ, Israel L, Watanabe S, Hochheimer A, Peterson CL, Korber P

Supplementary Figures S1-S8

Supplementary Tables S1, S3 and S4

Supplementary Materials and Methods

Supplementary References

Supplementary Figures

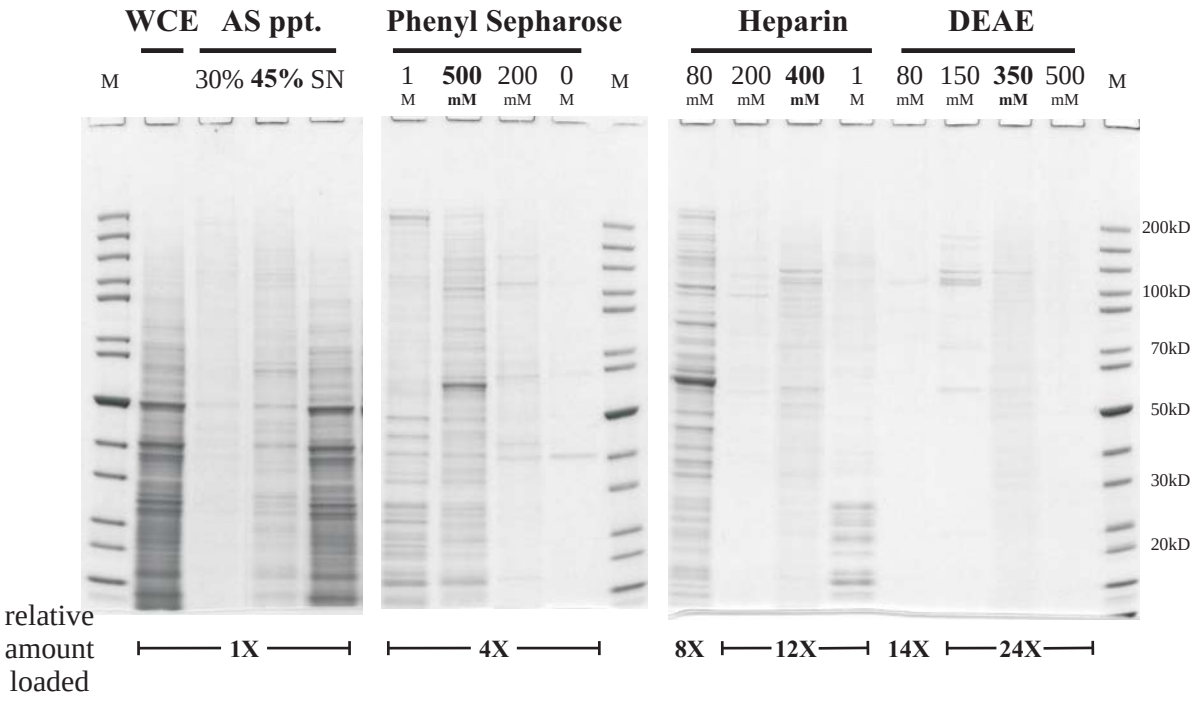

Supplementary Figure S1 Fractionation of the yeast whole cell extract over four sequential steps removes a majority of proteins. Analysis of the protein content of WCE and fractions obtained from each purification step as in Figure 1B on a 4-12% acrylamide SDS gel stained with colloidal coomassie. 1 µl of WCE was loaded and the relative amount indicated below the lanes of the fractions, such that the volume increase relative to input was compensated. Fractions positive for the *PHO8* promoter nucleosome positioning activity are labeled in bold. Sizes of some marker bands are indicated on the right. AS ppt., ammonium sulphate precipitation. SN, supernatant.

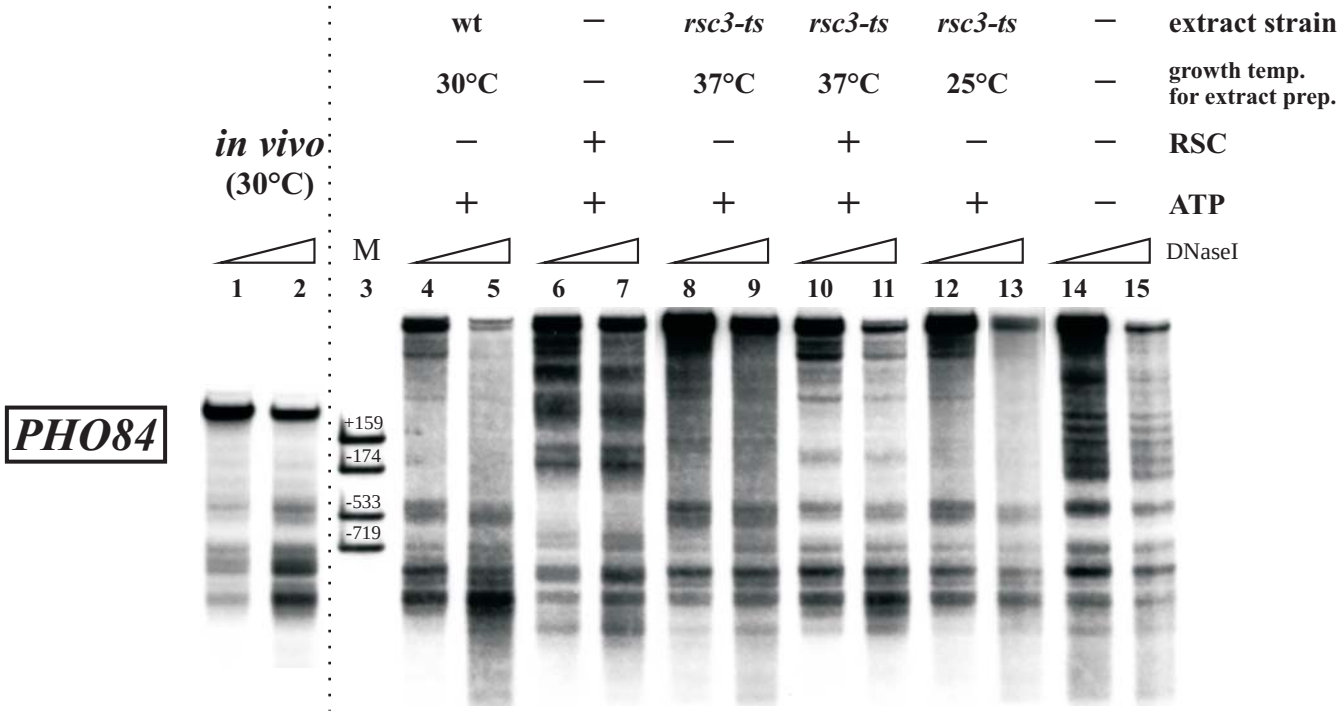

Supplementary Figure S2 The *in vivo*-like positioning at the *PHO84* promoter generated by salt gradient dialysis assembly is counteracted by RSC alone but not in the context of the *rsc3-ts* 37 °C extract. As Figure 3, but with plasmid pUC19-*PHO84*. The *in vivo* sample was electrophoresed on a separate gel as indicated by the stippled line. For the *in vivo* sample secondary cleavage was with HindIII instead of SspI so that the top band migrates lower in the lane.

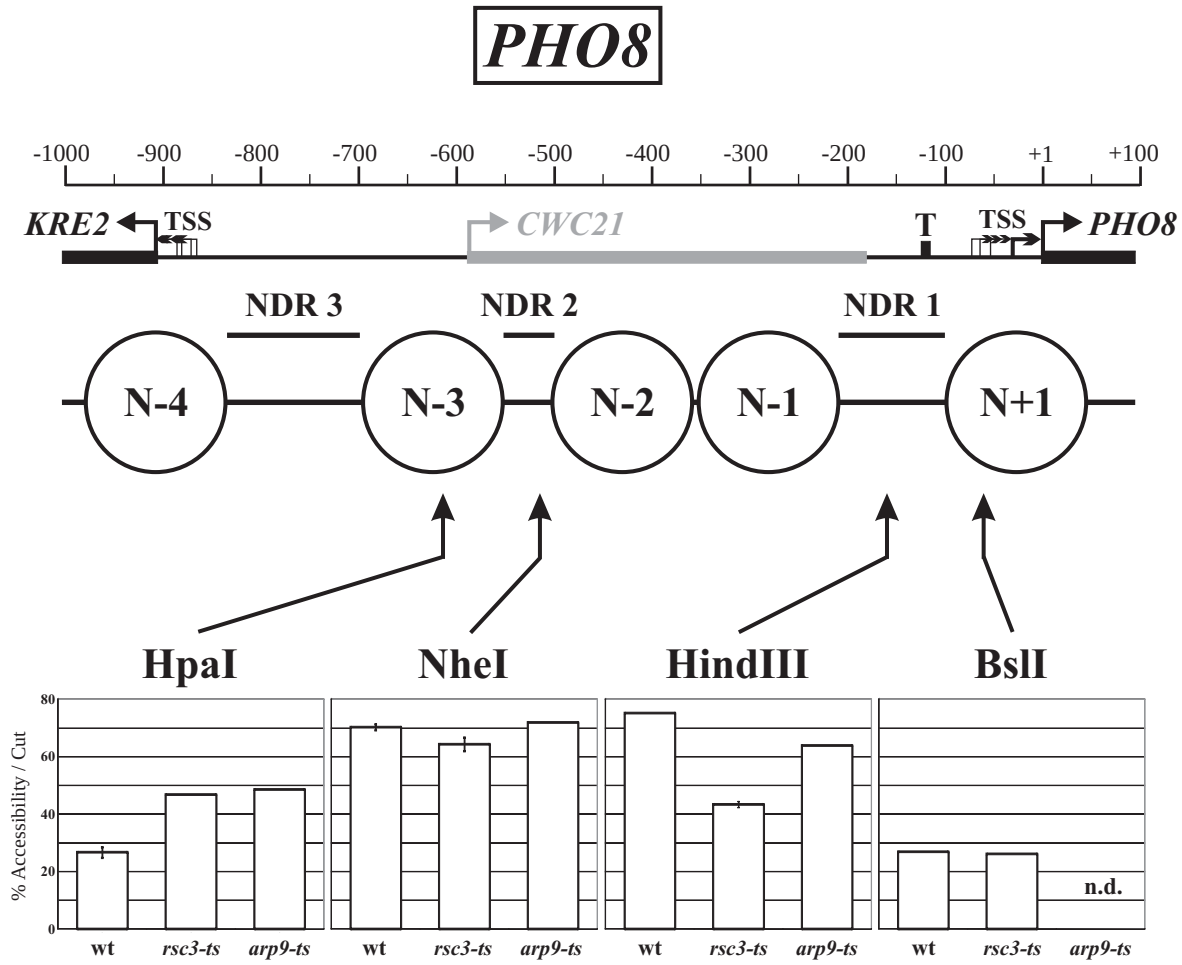

Supplementary Figure S3 Ablation of RSC subunits changed restriction enzyme accessibilities at the *PHO8* promoter. Nuclei isolated from wildtype (wt; BY4741) and ts (*rsc3-ts* (TH8247) and *arp9-ts* (YBC1536)) strains as in Figure 5 after overnight incubation at 37 °C were digested with the indicated restriction enzymes. Schematics of the *PHO8* promoter as in Figure 1A. Arrows indicate the position of the corresponding restriction site. Error bars show the variation of two biological replicates. n.d. not determined.

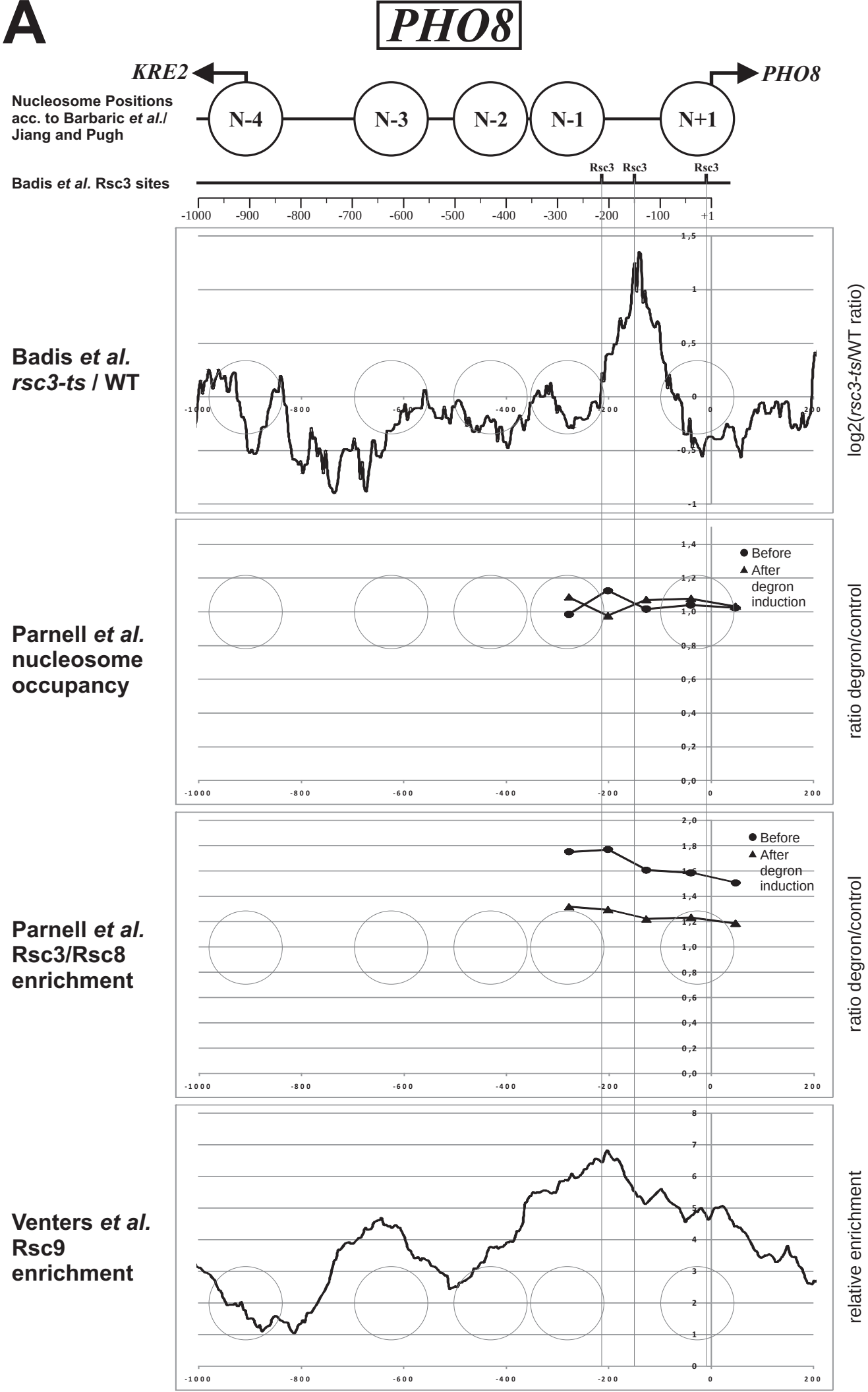
A
PHO8
KRE2
PHO8
Nucleosome Positions acc. to Barbaric et al./ Jiang and Pugh
N-4
N-3
N-2
N-1
N+1
Badis et al. Rsc3 sites
Rsc3
Rsc3
Rsc3
-1000
-900
-800
-700
-600
-500
-400
-300
-200
-100
+1
Badis et al. rsc3-ts / WT
log2(rsc3-ts/WT ratio)
Parnell et al. nucleosome occupancy
Before
After degron induction
ratio degron/control
Parnell et al. Rsc3/Rsc8 enrichment
Before
After degron induction
ratio degron/control
Venters et al. Rsc9 enrichment
relative enrichment

B

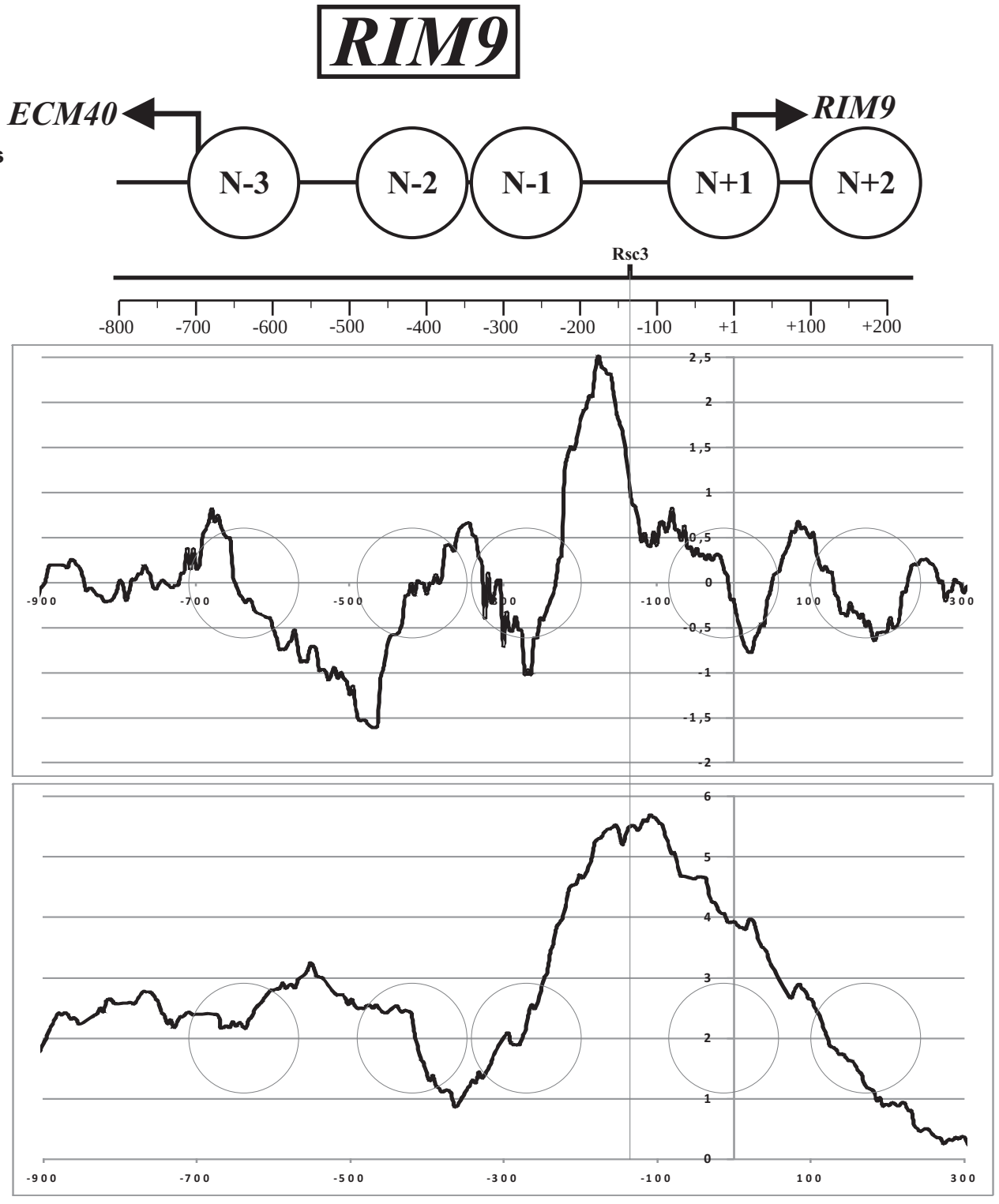
RIM9
ECM40
RIM9
N-3
N-2
N-1
N+1
N+2
Nucleosome Positions according to Jiang and Pugh
Badis et al. Rsc3 sites
Rsc3
-800
-700
-600
-500
-400
-300
-200
-100
+1
+100
+200
Badis et al. rsc3-ts / WT
log2(rsc3-ts/WT ratio)
Venters et al. Rsc9 enrichment
relative enrichment

C

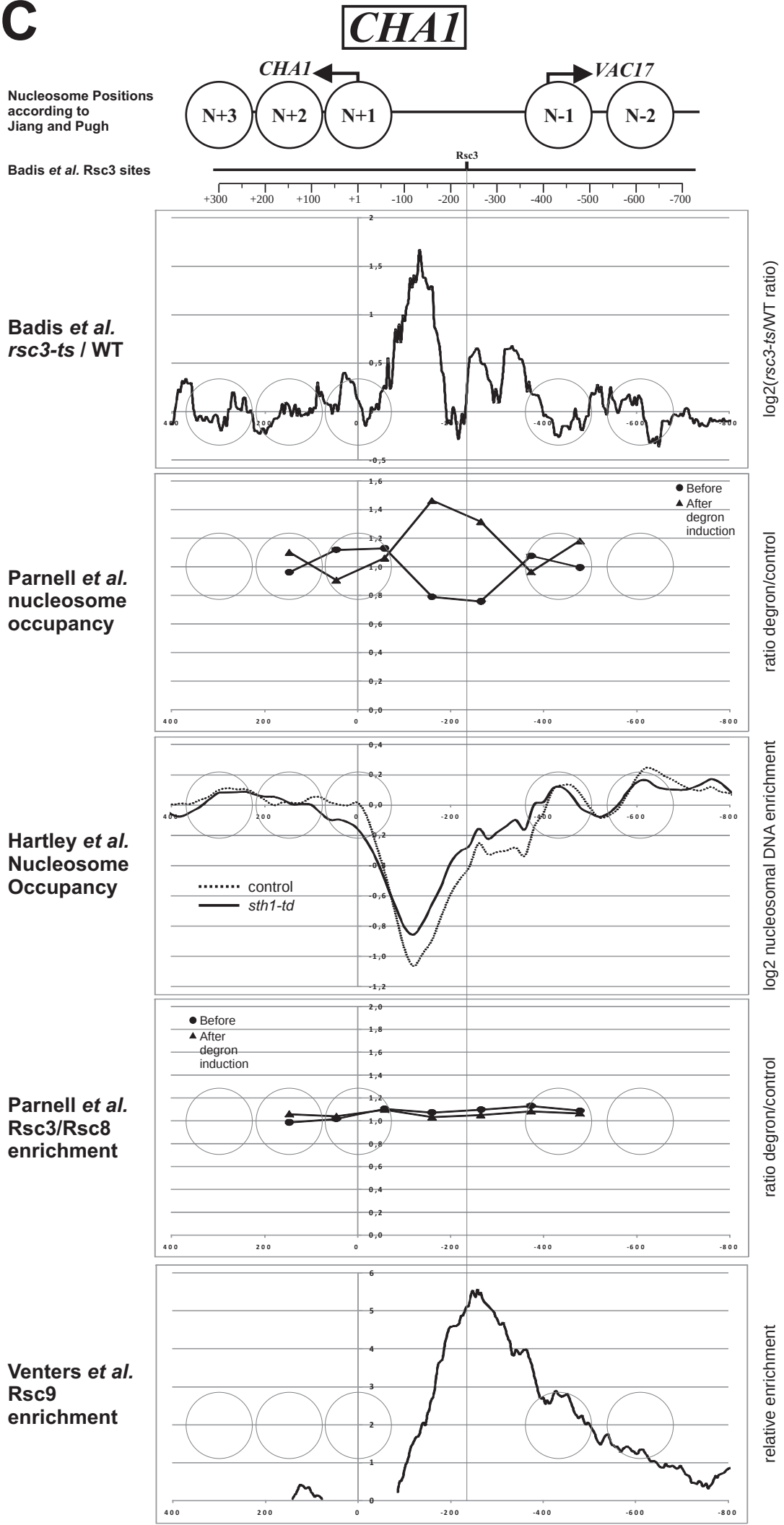
CHA1
CHA1
VAC17
Nucleosome Positions according to Jiang and Pugh
N+3
N+2
N+1
N-1
N-2
Badis et al. Rsc3 sites
Rsc3
+300 +200 +100 +1 -100 -200 -300 -400 -500 -600 -700
Badis et al. rsc3-ts / WT
log2(rsc3-ts/WT ratio)
Parnell et al. nucleosome occupancy
Before
After degron induction
ratio degron/control
Hartley et al. Nucleosome Occupancy
control
sth1-td
log2 nucleosomal DNA enrichment
Parnell et al. Rsc3/Rsc8 enrichment
Before
After degron induction
ratio degron/control
Venters et al. Rsc9 enrichment
relative enrichment

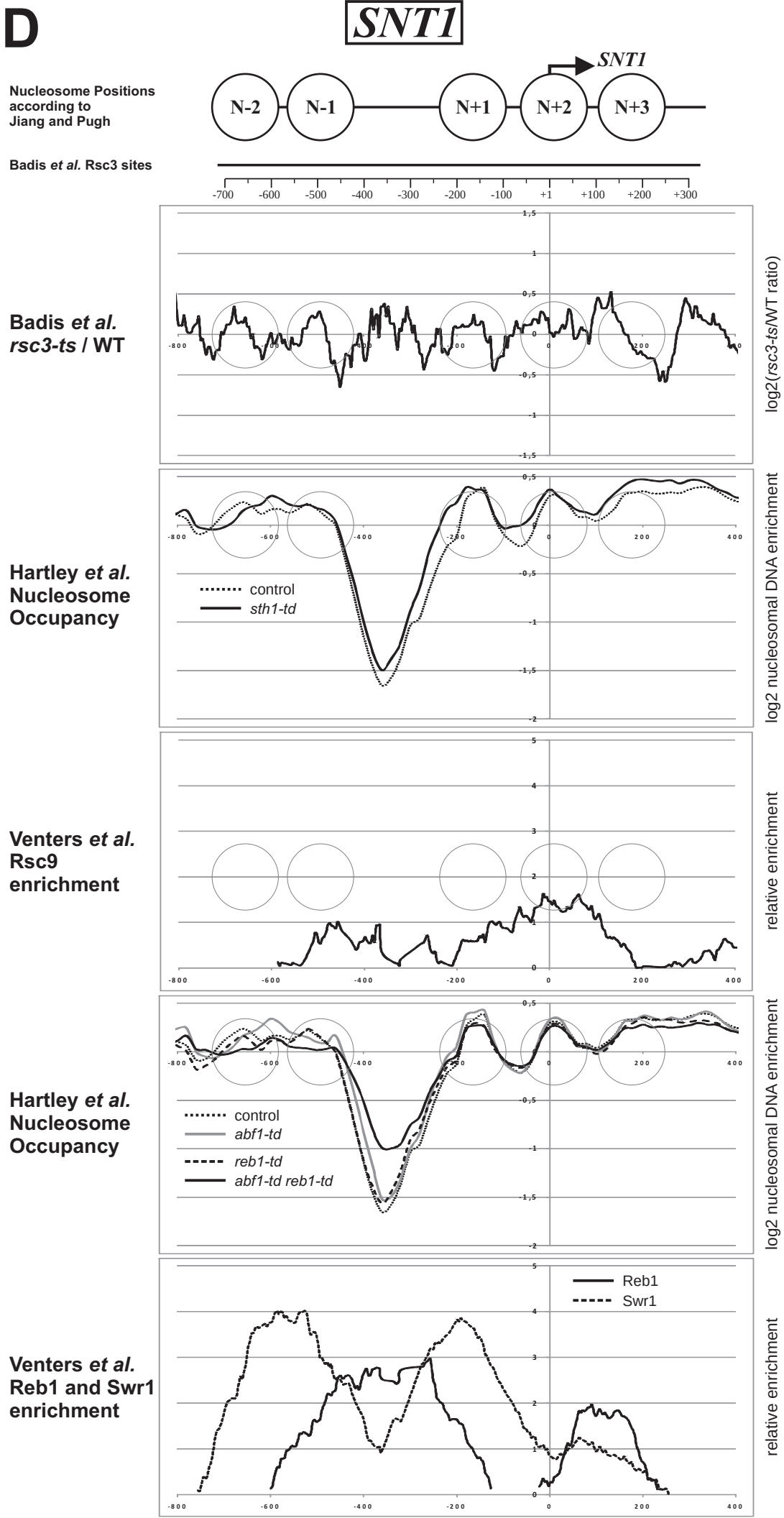
D
SNT1
SNT1
Nucleosome Positions according to Jiang and Pugh
N-2
N-1
N+1
N+2
N+3
Badis et al. Rsc3 sites
-700 -600 -500 -400 -300 -200 -100 +1 +100 +200 +300
Badis et al. rsc3-ts / WT
log2(rsc3-ts/WT ratio)
Hartley et al. Nucleosome Occupancy
control
sth1-td
log2 nucleosomal DNA enrichment
Venters et al. Rsc9 enrichment
relative enrichment
Hartley et al. Nucleosome Occupancy
control
abf1-td
reb1-td
abf1-td reb1-td
log2 nucleosomal DNA enrichment
Venters et al. Reb1 and Swr1 enrichment
Reb1
Swr1
relative enrichment

E

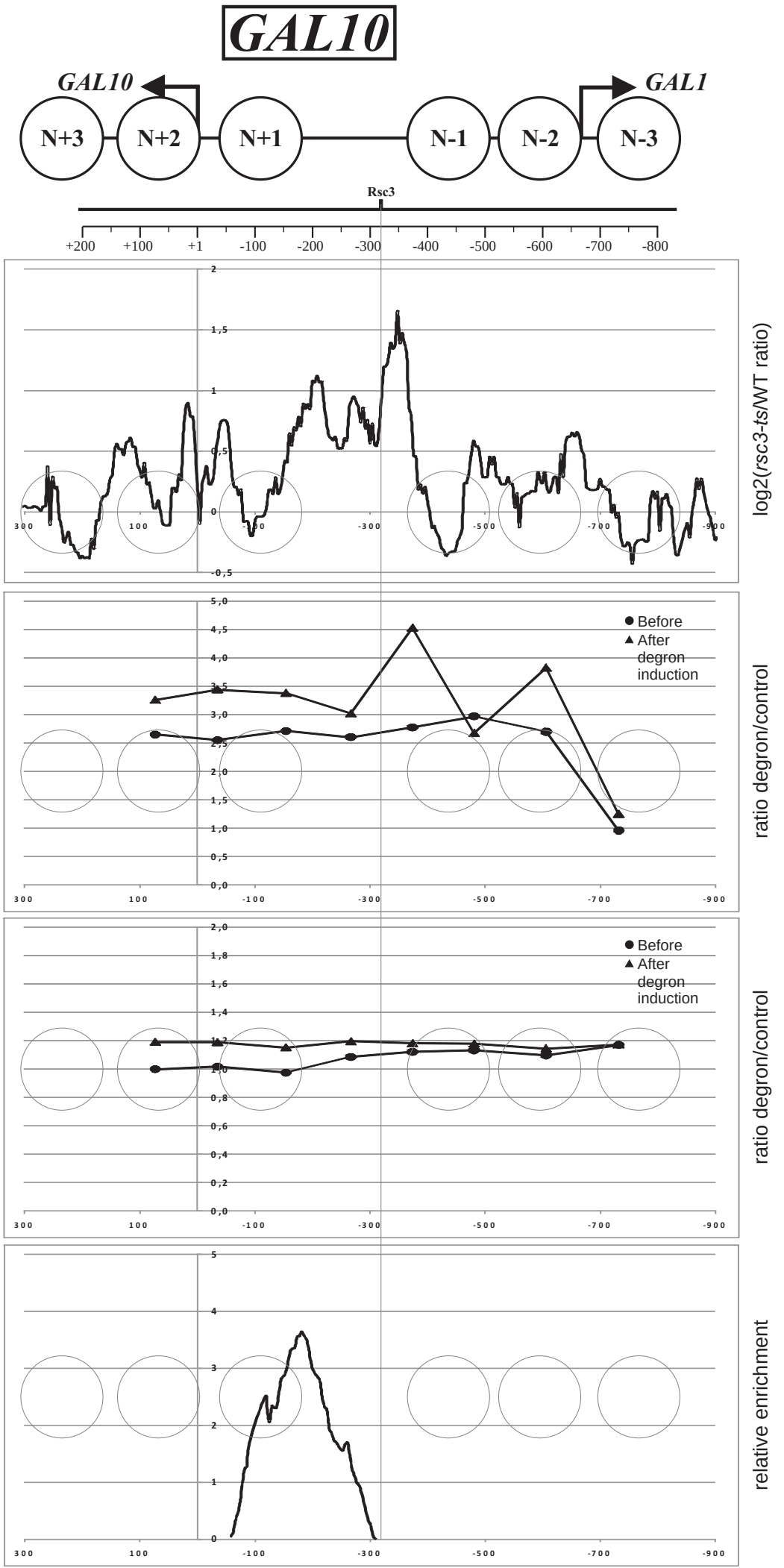
GAL10
GAL10
GAL1
N+3
N+2
N+1
N-1
N-2
N-3
Nucleosome Positions according to Jiang and Pugh
Badis et al. Rsc3 sites
Rsc3
+200
+100
+1
-100
-200
-300
-400
-500
-600
-700
-800
Badis et al. rsc3-ts / WT
log2(rsc3-ts/WT ratio)
Parnell et al. nucleosome occupancy
Before
After degron induction
ratio degron/control
Parnell et al. Rsc3/Rsc8 enrichment
Before
After degron induction
ratio degron/control
Venters et al. Rsc9 enrichment
relative enrichment

F

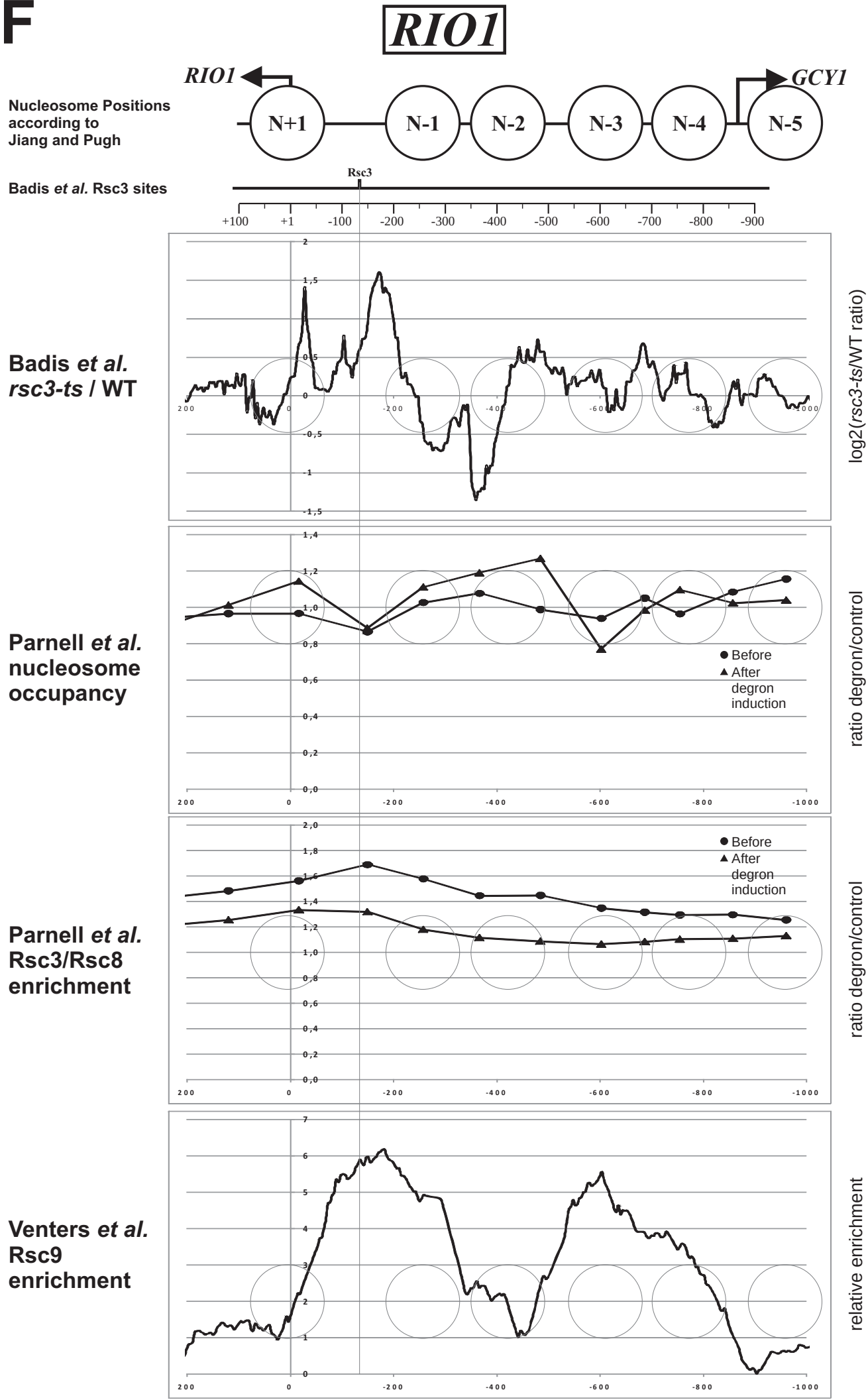
RIO1
RIO1
GCY1
Nucleosome Positions according to Jiang and Pugh
N+1
N-1
N-2
N-3
N-4
N-5
Badis et al. Rsc3 sites
Rsc3
+100
+1
-100
-200
-300
-400
-500
-600
-700
-800
-900
Badis et al. rsc3-ts / WT
log2(rsc3-ts/WT ratio)
Parnell et al. nucleosome occupancy
Before
After degron induction
ratio degron/control
Parnell et al. Rsc3/Rsc8 enrichment
Before
After degron induction
ratio degron/control
Venters et al. Rsc9 enrichment
relative enrichment

G

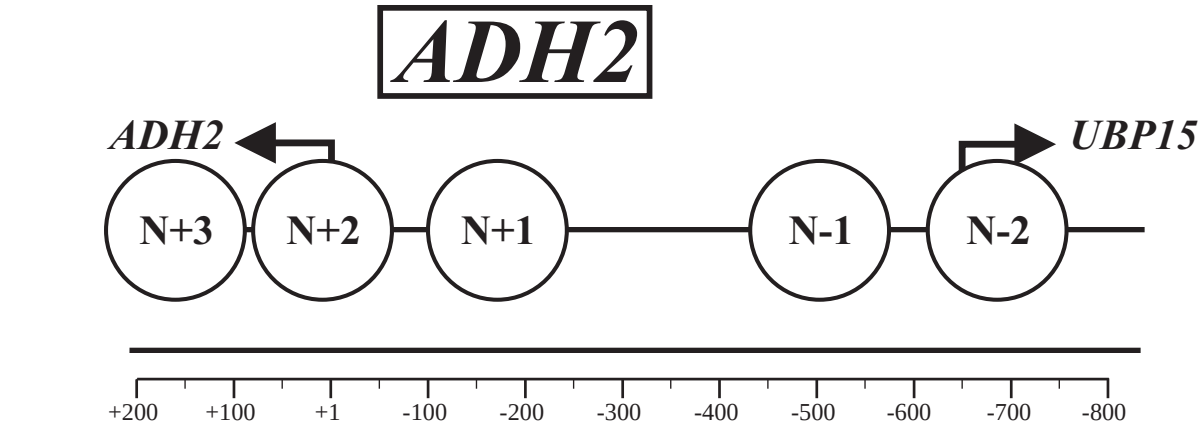

Nucleosome Positions according to Jiang and Pugh

Badis *et al.* Rsc3 sites

Badis *et al.* *rsc3-ts* / WT

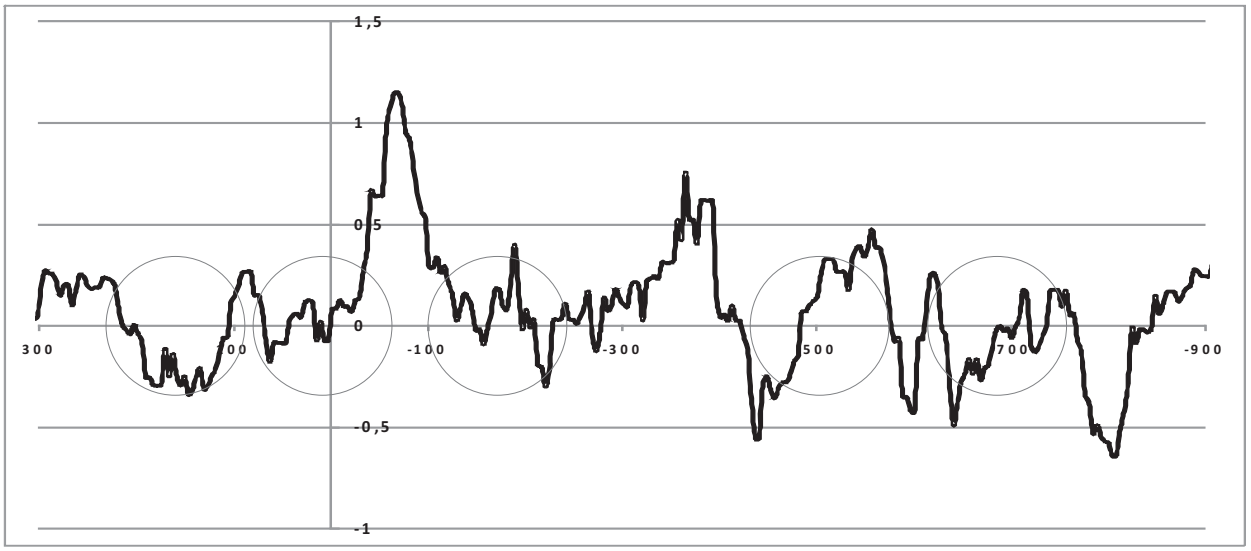

Venters *et al.* Rsc9 enrichment

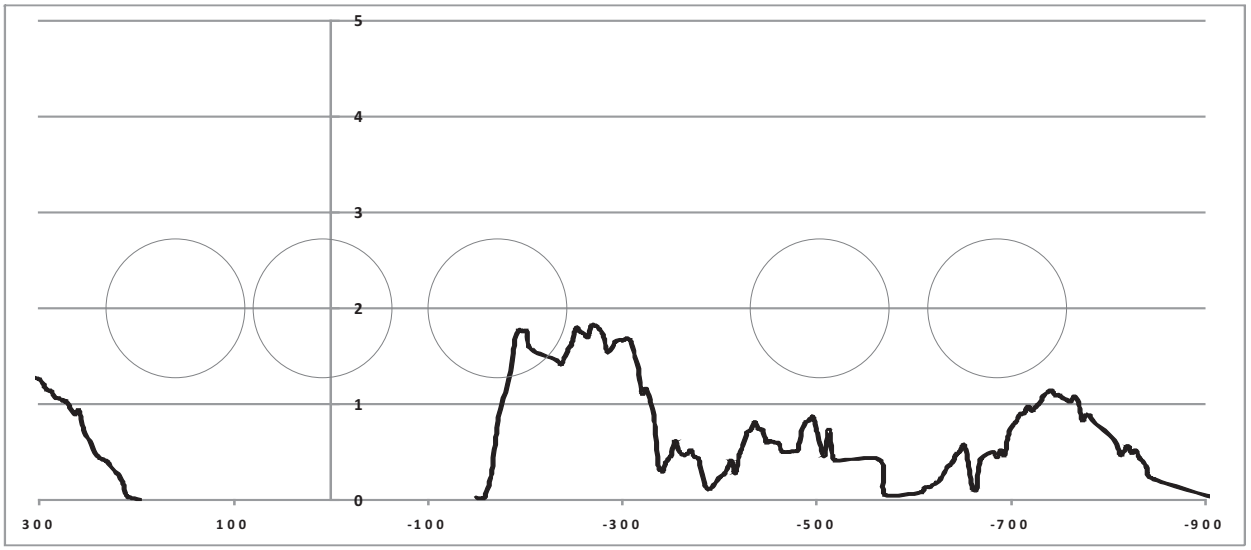

H

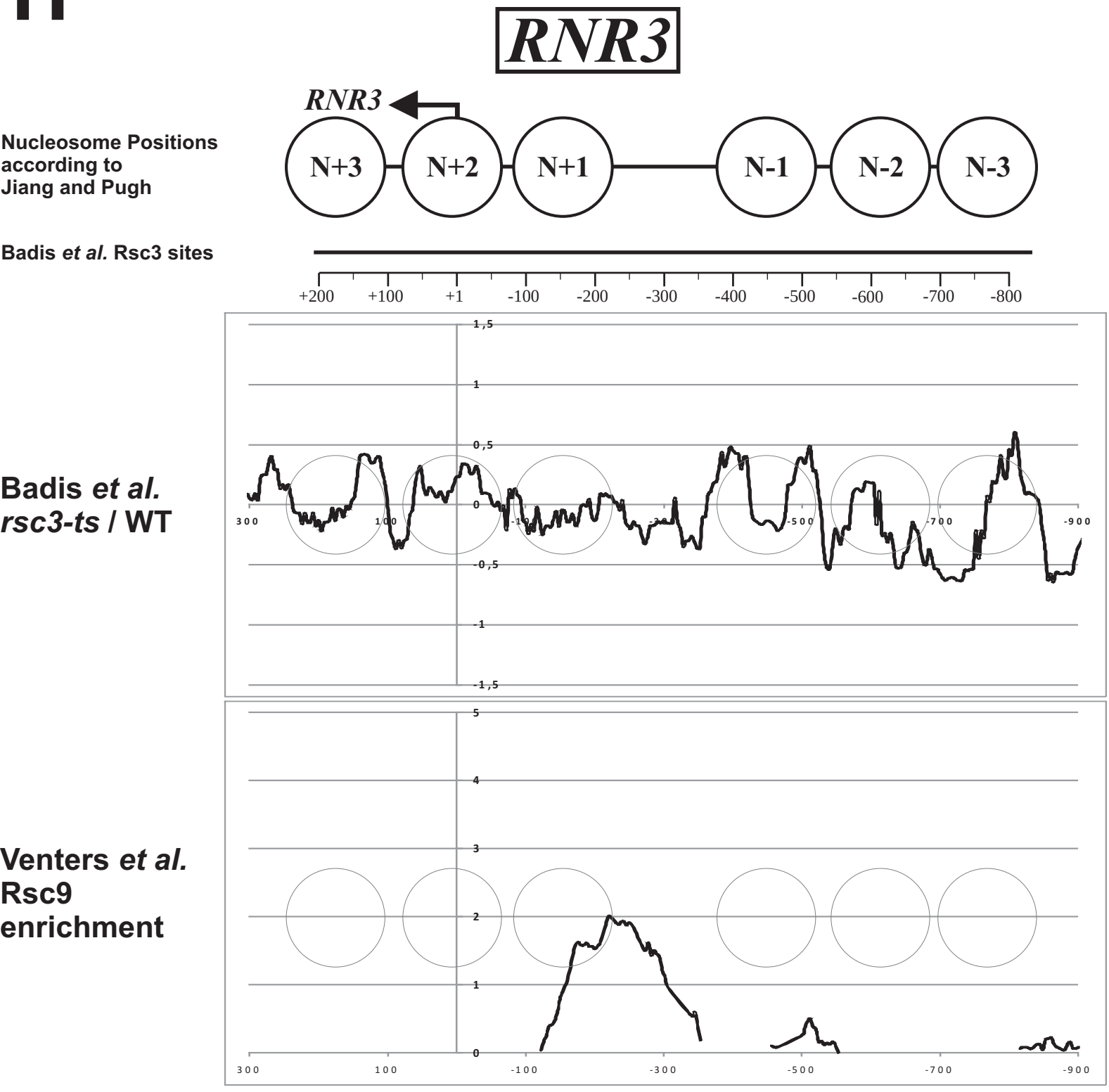
RNR3
RNR3
Nucleosome Positions according to Jiang and Pugh
N+3
N+2
N+1
N-1
N-2
N-3
Badis et al. Rsc3 sites
+200
+100
+1
-100
-200
-300
-400
-500
-600
-700
-800
Badis et al. rsc3-ts / WT
1,5
1
0,5
0
-0,5
-1
-1,5
300
100
-500
-700
-900
log2(rsc3-ts/WT ratio)
Venters et al. Rsc9 enrichment
5
4
3
2
1
0
300
100
-100
-300
-500
-700
-900
relative enrichment

I

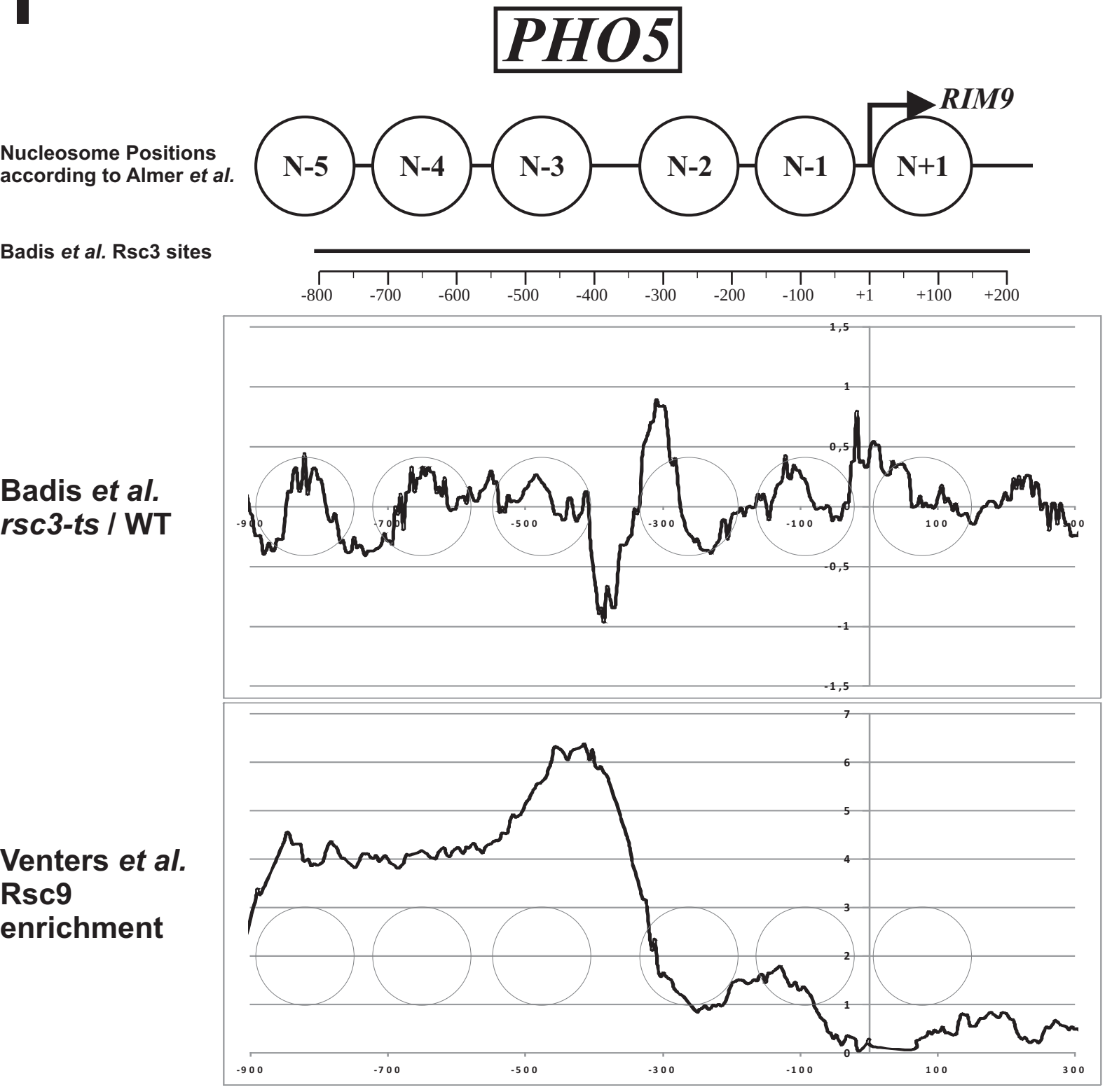
PHO5
RIM9
Nucleosome Positions according to Almer et al.
N-5
N-4
N-3
N-2
N-1
N+1
Badis et al. Rsc3 sites
-800
-700
-600
-500
-400
-300
-200
-100
+1
+100
+200
Badis et al. rsc3-ts / WT
1,5
1
0,5
0
-0,5
-1
-1,5
-900
-700
-500
-300
-100
100
300
log2(rsc3-ts/WT ratio)
Venters et al. Rsc9 enrichment
7
6
5
4
3
2
1
0
-900
-700
-500
-300
-100
100
300
relative enrichment

J

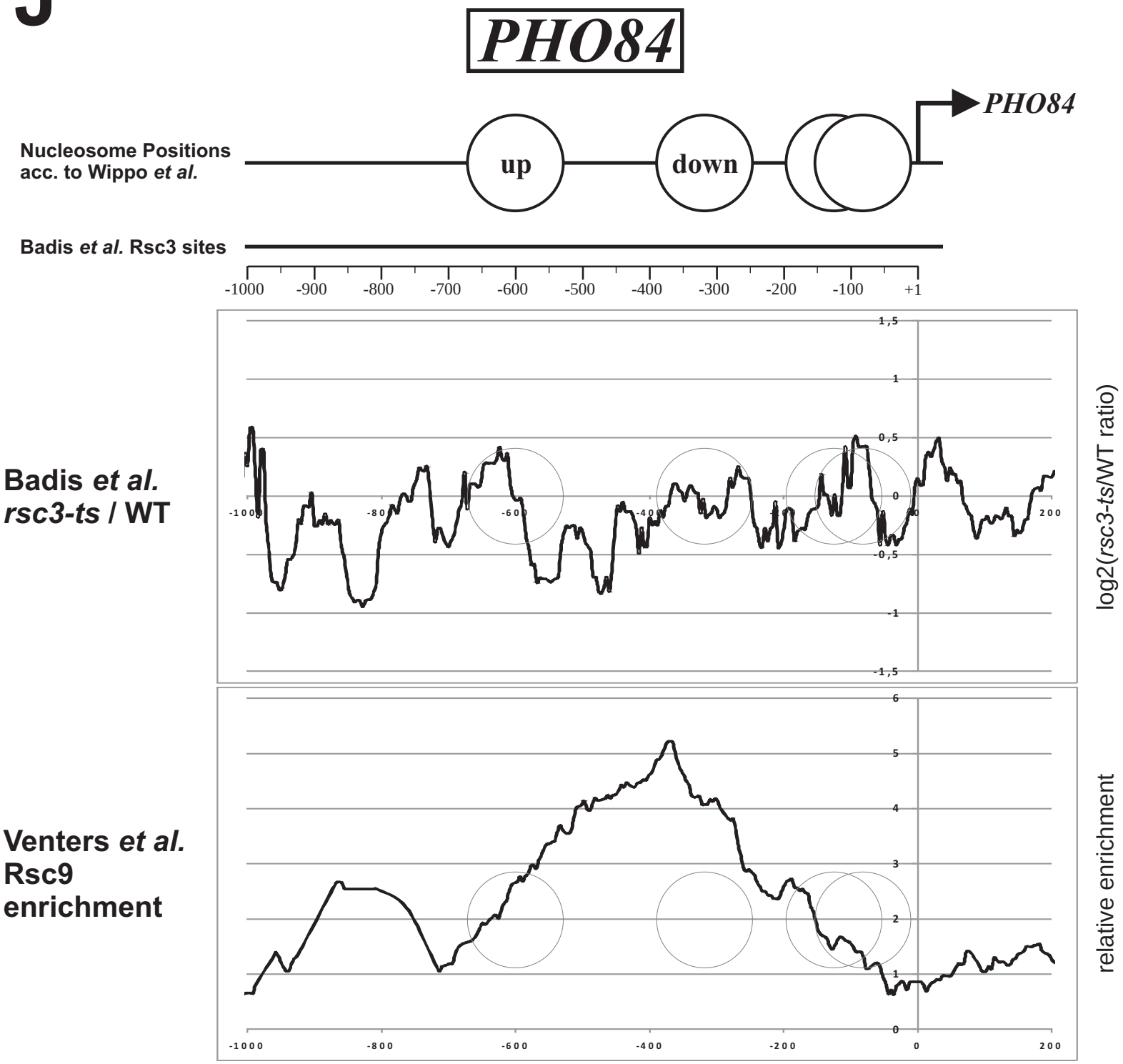

Supplementary Figure S4 Comparison of the available datasets on RSC localization and effects on nucleosome occupancy upon ablation of RSC subunits. (**A-J**) The Schematics at the top indicate the position of the nucleosomes (according to Jiang and Pugh (2009) unless stated otherwise) and the ORF starts (broken arrows). Putative Rsc3 binding sites as identified using the Badis et al. (2008) PWM are shown in the panel below. The graphs below the schematics show nucleosome occupancy changes in a *rsc3-ts* strain (Badis et al. (2008)) and *sth1-td* strains (Parnell et al. (2008) and Hartley and Madhani (2009)) as well as RSC occupancy profiles obtained by Parnell et al. (2008) and Venters et al. (2009) as indicated. For some loci only limited amounts of data were available, since the microarray of Parnell et al. only included selected promoters and the microarray of Hartley et al. was limited to chromosome III. Gaps in the Venters et al. Rsc9 profile correspond to unavailable data for the corresponding regions.

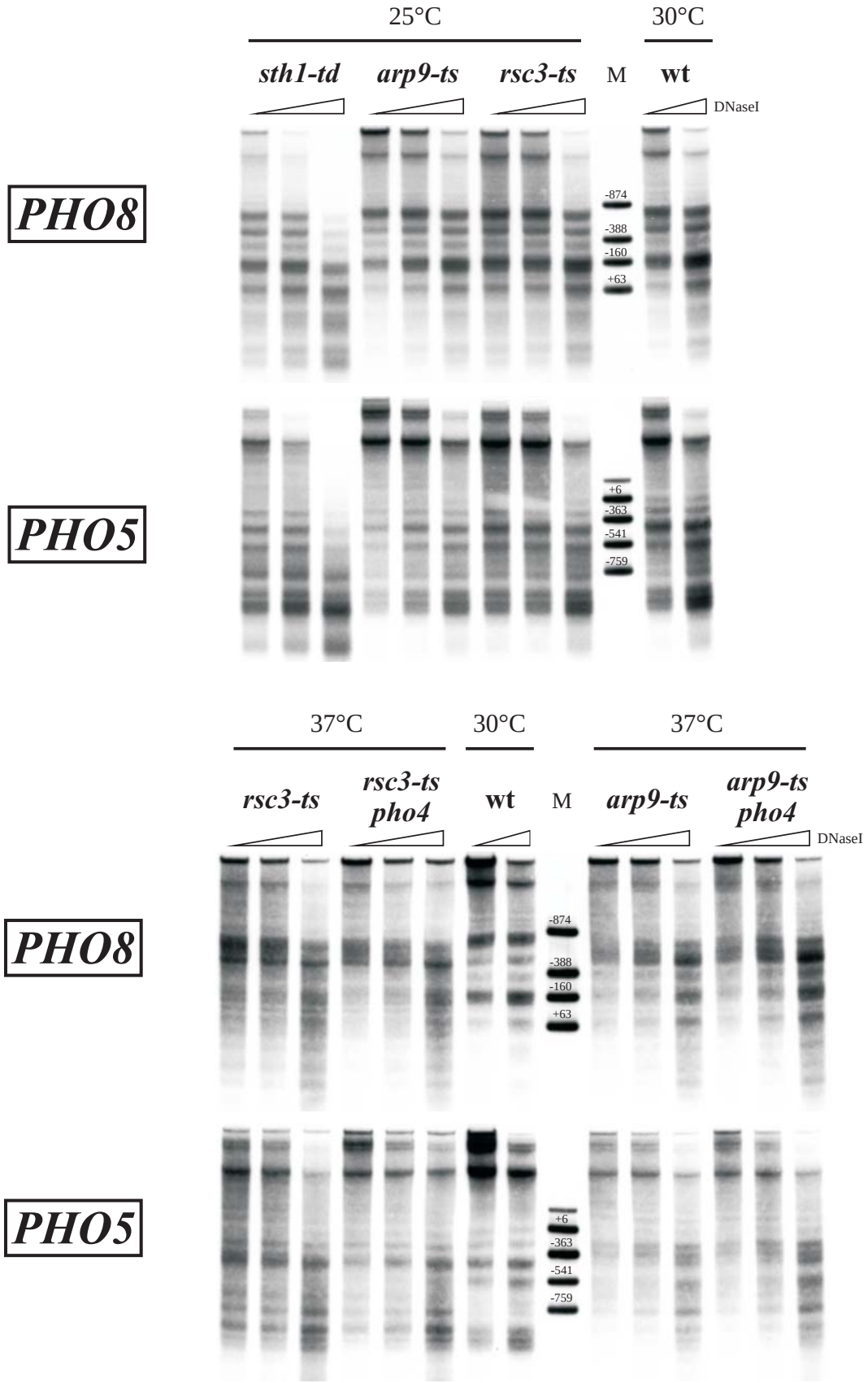

Supplementary Figure S5 Changes in *PHO8* promoter chromatin upon loss of Rsc3 or Arp9 were Pho4-independent and only seen at the non-permissive temperature. As Figure 5, but for the indicated loci, strains and growth conditions, i.e., either logarithmic growth at 25 °C or 30 °C or logarithmic growth at 25 ° and then shifted to 37 °C overnight.

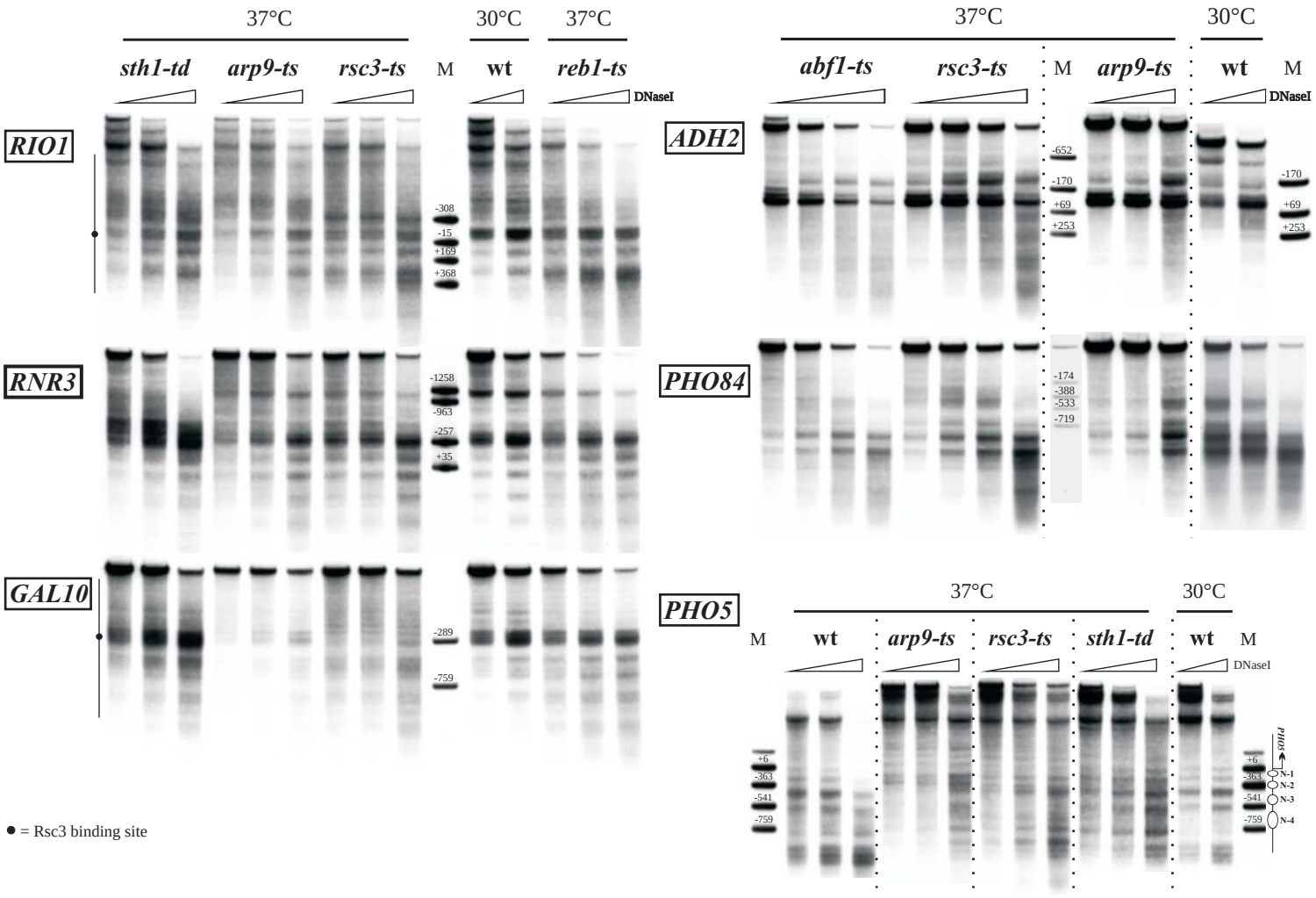

Supplementary Figure S6 Changes of the chromatin structure upon RSC inactivation at the *RIO1*, *RNR3*, *GAL10*, *ADH2*, *PHO84*, and *PHO5* promoters. As Figure 5, but for the indicated loci. Strains with temperature sensitive alleles of the genes encoding Reb1 or Abf1 (TH8242 and TH8246, respectively) grown under restrictive conditions are included for some loci. As there were no effects in these strains, they serve as negative control for the growth conditions.

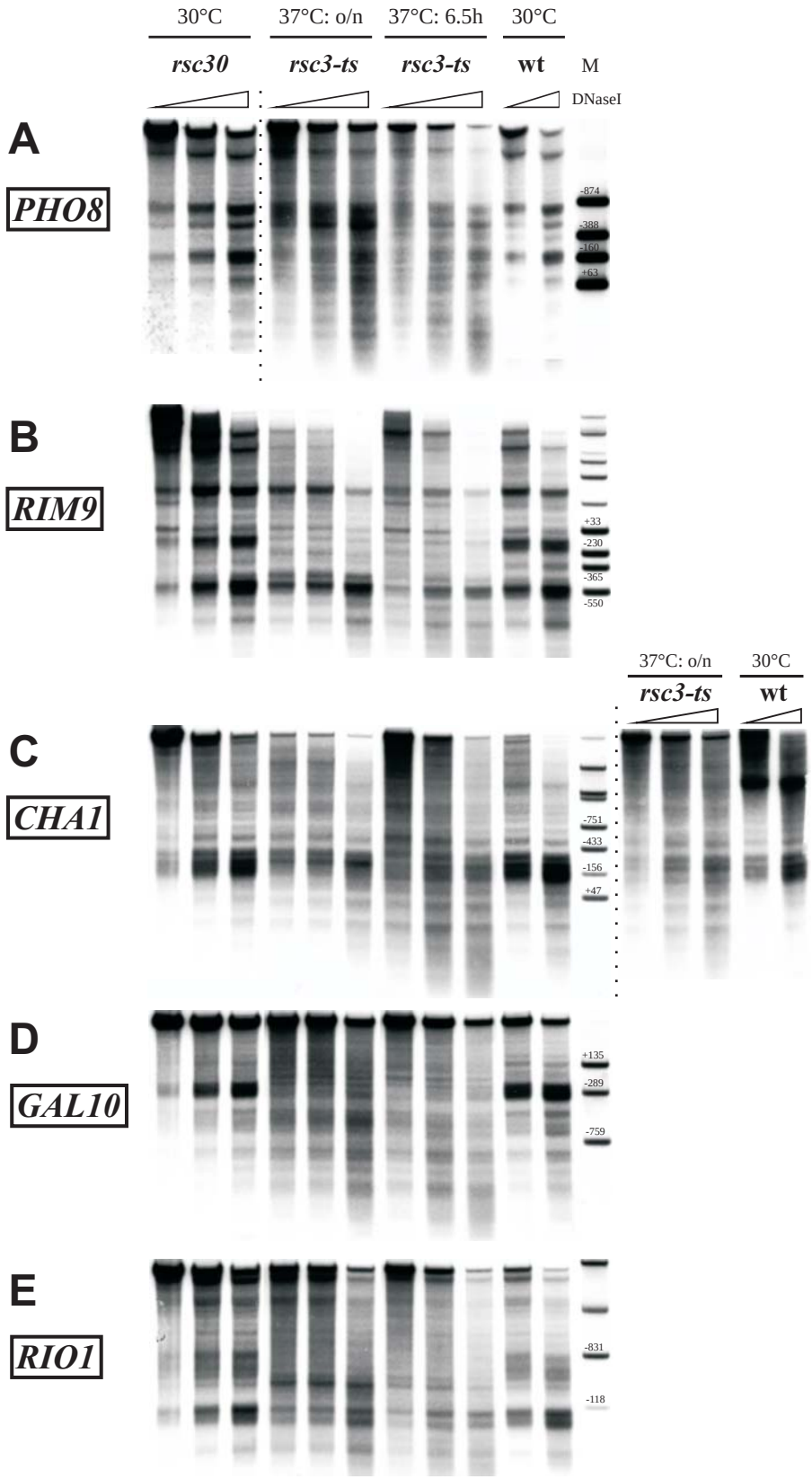

Supplementary Figure S7 Also shorter incubation times at the restrictive temperature showed the altered chromatin structures at the *PHO8*, *RIM9*, *CHA1*, *GAL10* and *RIO1* promoters in the *rsc3-ts* strain. DNaseI indirect end labeling analysis of the (**A**) *PHO8*, (**B**) RIM9, (**C**) *CHA1* (**D**) *GAL10* and (**E**) *RIO1* promoter regions *in vivo*. Nuclei were isolated from a wildtype strain (wt; BY4741), a strain carrying the deletion mutant allele *rsc30* (YBC693) and the *rsc3-ts* (TH8247) mutant. Strains were grown either grown logarithmically at 30°C, or at 25 °C and then shifted to the non-permissive temperature (37 °C) for 6.5h as done by Badis et al. (2008) or overnight. The results for the *CHA1* locus in lanes 4 to 6 and lanes 10 to 12 are the same as in Figure 5C. In addition, results of an experiment where there was not much difference between the wt and the *rsc3-ts* mutant after overnight incubation at 37 °C is shown on the right to the stippled line in panel (**C**). A stippled line separates samples that were not electrophoresed alongside on the same gel but combined in the figure. Ramps, markers and schematics as in Figure 4.

A ***PHO8***

	Rsc3 site at -10	Rsc3 site at -151	Rsc3 site at -214
S.cerevisiae	**C G C G C** A T	T **C G C G C G** T	A G **G C G C G**
S.paradoxus	**C G C G C** A T	T **C G C G C G** T	A G **G C G C G**
S.mikatae	**C G C G C** A T	T **C G C G C G** T	A G **G C G C G**
S.bayanus	T A A G C A T	T **C G C G C G** T	A G **G C G C G**
S.kudriavzevii	C T A G C A T	T **C G C G C G** T	A G **G C G C G**
S.castelli	A G A G T A A	G T A C A C A G	C C A C T C G

B

	RIM9	***CHA1***	***GAL10***	***RIO1***
	Rsc3 site at -133	**Rsc3 site at -239**	**Rsc3 site at -214**	**Rsc3 site at -134**
S.cerevisiae	C G **G C G C G C G C** A A	C T **G C G C G**	C G **G C G C G**	T G **G C G C G C G C** A G
S.paradoxus	C G **G C G C G C G C** T A	T T T C G T G	C G **G C G C G**	T A **G C G C G C G C** A G
S.mikatae	C G **G C G C G C** C T A A	C T **G C G C G**	T G G T G C G	T A **G C G C G C G C** A A
S.bayanus	C G **G C G C G C** A A G A	C C G T G C G	C G **G C G C G**	C A T **C G C G C G** A C G
S.kudriavzevii	C G **G C G C G C G C** A A	C **C G C G C G**	- - - - - - -	T A G C G C C C G A C G
S.castelli	T G **G C G C G** T A T G T	A G C G G T G	C T T C A T C	A A G T C A G T A C A G
S.kluyveri	T C G C A T A A T T A A	G C T C T T T	- - - - - - -	- - - - - - - - - - - - -

***SNT1, PHO5, ADH2, RNR3, PHO84*: no predicted Rsc3 binding site**

Supplementary Figure S8 Evolutionary conservation of Rsc3 binding sites at various loci. (**A**) Sequence alignment of three predicted Rsc3 sites at the *PHO8* promoter in the indicated *Saccharomyces* species. CGCGC consensus motif in bold and cross-species conservation marked by black dots. (**B**) As (**A**), but for the indicated loci.

Supplementary Table S1 Yeast strains used in this study.

Strain	Genotype	Reference
Y00000 (BY4741)	MATa his3Δ1 leu2Δ0 met15Δ0 ura3Δ0	EUROSCARF http://web.uni-frankfurt.de/fb15/mikro/euroscarf/
Y00397	MATa his3Δ1 leu2Δ0 met15Δ0 ura3Δ0 scw3::kanMX4	
Y00994	MATa his3Δ1 leu2Δ0 met15Δ0 ura3Δ0 rrm3::kanMX4	
Y01076	MATa his3Δ1 leu2Δ0 met15Δ0 ura3Δ0 ypl216w::kanMX4	
Y01285	MATa his3Δ1 leu2Δ0 met15Δ0 ura3Δ0 rpb4::kanMX4	
Y01343	MATa his3Δ1 leu2Δ0 met15Δ0 ura3Δ0 scp160::kanMX4	
Y01514	MATa his3Δ1 leu2Δ0 met15Δ0 ura3Δ0 hsp104::kanMX4	
Y01655	MATa his3Δ1 leu2Δ0 met15Δ0 ura3Δ0 hap5::kanMX4	
Y02123	MATa his3Δ1 leu2Δ0 met15Δ0 ura3Δ0 taf14::kanMX4	
Y03092	MATa his3Δ1 leu2Δ0 met15Δ0 ura3Δ0 sef1::kanMX4	
Y03418	MATa his3Δ1 leu2Δ0 met15Δ0 ura3Δ0 sgf29::kanMX4	
Y03648	MATa his3Δ1 leu2Δ0 met15Δ0 ura3Δ0 rtt103::kanMX4	
Y04196	MATa his3Δ1 leu2Δ0 met15Δ0 ura3Δ0 eaf1::kanMX4	
Y05326	MATa his3Δ1 leu2Δ0 met15Δ0 ura3Δ0 cdc73::kanMX4	
Y05347	MATa his3Δ1 leu2Δ0 met15Δ0 ura3Δ0 hda1::kanMX4	
Y05727	MATa his3Δ1 leu2Δ0 met15Δ0 ura3Δ0 paf1::kanMX4	
Y05922	MATa his3Δ1 leu2Δ0 met15Δ0 ura3Δ0 yta7::kanMX4	
Y05927	MATa his3Δ1 leu2Δ0 met15Δ0 ura3Δ0 rtt102::kanMX4	
Y06520	MATa his3Δ1 leu2Δ0 met15Δ0 ura3Δ0 yml199w::kanMX4	
Y06546	MATa his3Δ1 leu2Δ0 met15Δ0 ura3Δ0 yku80::kanMX4	
Y06566	MATa his3Δ1 leu2Δ0 met15Δ0 ura3Δ0 sto1::kanMX4	

Supplementary Table S1 - continued

Strain	Genotype	Reference
TH8242	MATa his3Δ1 leu2Δ0 met15Δ0 ura3Δ0 abf1-101::KanMX	Badis et al. 2008
TH8245	MATa his3Δ1 leu2Δ0 met15Δ0 ura3Δ0 rap1-1::KanMX	
TH8246	MATa his3Δ1 leu2Δ0 met15Δ0 ura3Δ0 KanMX::reb1-212-URA3	
TH8247 (= *rsc3-ts*)	MATa his3Δ1 leu2Δ0 met15Δ0 ura3Δ0 rsc3-1::KanMX	
TH8239	MATa his3Δ1 leu2Δ0 met15Δ0 ura3Δ0 rsc3-1::kanMX rsc8-TAP::HIS3MX6	
YBC693	MATa ade2Δ::hisG his3Δ200 leu2Δ0 lys2Δ0 met15Δ0 trp1Δ63 ura3Δ0 rsc30Δ::LEU2	Angus-Hill et al. 2001
YBC1536 (= *arp9-ts*)	MATa lys2-128δ leu2Δ1 ura3-52 trp1Δ63 his3Δ200 arp9Δ::LEU2 [p1014; arp9 G337F G338L; CEN TRP1]	Szerlong et al. 2003
YBC2191 (= *sth1-td*)	MATa ura3-52 trp1Δ63 his3Δ200 leu2::PET56 ubr1Δ::pGAL1-UBR::HIS3 sth1Δ::pCUP1-sth1^{td}::URA3	Parnell et al. 2008
YBC2192	MATa ura3-52 trp1Δ63 his3Δ200 leu2::PET56 ubr1Δ::HIS3 sth1Δ::pCUP1-sth1^{td}::URA3	
arp9-ts pho4	MATa lys2-128δ leu2Δ1 ura3-52 trp1Δ63 his3Δ200 arp9Δ::LEU2 pho4Δ::URA3 [p1014;arp9 G337F G338L; CEN TRP1]	This work
rsc3-ts pho4	MATa his3Δ1 leu2Δ0 met15Δ0 ura3Δ0 rsc3-1::KanMX pho4Δ::URA3	This work
FY2810	MATa leu2Δ1 his4-912δ lys2-128δ FLAG-spt6-1004	F.Winston

	Subunit(s) tested	*PHO8*	*RIM9*	*CHA1*	*SNT1*	*GAL10*	*RIO1*	*ADH2*	*RNR3*	*PHO5*	*PHO84*
		Changes in nucleosome occupancy/positioning upon inactivation of RSC subunits									
Wippo *et al.*	**Sth1/Rsc3/Arp9**	+ + +	+ + +	- (+) (-)	- - -	- + (-)	(-) + (+)	n.d. - -	+ - -	- (+) +	n.d. - -
Badis *et al.*	**Rsc3**	+	+	+	-	+	+	(+)	-	(+)	-
Parnell *et al.*	**Sth1**	-	n.d.	+	n.d.	+	(-)	n.d.	n.d.	n.d.	n.d.
Hartley and Madhani	**Sth1**	n.d.	n.d.	(+)	-	n.d.	n.d.	n.d.	n.d.	n.d.	n.d.
		RSC-bound nucleosomes at the promoter									
Floer *et al.*	**Rsc8**	+	-	-	-	+	-	-	-	-	-
		RSC occupancy									
Parnell *et al.*	**Rsc3/Rsc8**	+	n.d.	-	n.d.	-	+	n.d.	n.d.	n.d.	n.d.
Venters *et al.*	**Rsc9**	+	+	+	-	+	+	-	-	+	+
Ng *et al.*	**Rsc1/2/8, Sth1**	+	+	-	-	-	+	-	-	-	-
Damelin *et al.*	**Rsc9**	-	+	+	(-)	+	+	+	+	-	-

Supplementary Table S3 Overview comparison of our data (Wippo et al.) with data from the indicated sources for effects on nucleosome occupancy upon ablation of the indicated RSC subunit and for binding of the indicated RSC subunit (compare Supplementary Figure S4 and Supplementary Table S4). The table summarizes the respective data as following: +, clear effect/binding; -, no effect/binding; (+), weak effect; (-), very weak effect/binding; n.d., not determined.

Locus	Ng *et al.* (2002) RSC (Rsc1/2/8 and Sth1) occupancy (p-val)	Damelin *et al.*(2002) Rsc9 Occupancy (Median Percentile)	Floer *et al.* (2010) RSC/Nucleosome peaks (Location relative to ATG)
PHO8	**6.33E-08**	48.7	**-520** / **-269** / +362 / +1438
RIM9	**4.34E-05**	**93.0**	none
CHA1	5.88E-01	**96.4**	none
SNT1	7.18E-01	71.6	none
GAL10	3.18E-01	**94.5**	**-275** / +1002
RIO1	**1.27E-06**	**95.5**	+1251
ADH2	7.87E-01	**80.2**	+144 / +522 / +814
RNR3	1.03E-01	**86.4**	-652 / +191 / +488
PHO5	3.55E-01	37.1	+612
PHO84	5.99E-01	40.5	none

Supplementary Table S4 RSC binding scores obtained by Ng et al. (2002) (combined p-value for the Rsc1, Rsc2, Rsc3, Rsc8 and Sth1 ChIPs; significant values in bold) and Damelin et al. (2002) (promoters above the 71st / 72nd median percentile were classified as bound by RSC; significant values in bold) as well as the location of RSC-bound nucleosomes reported by Floer et al. (2010) (locations within promoter regions in bold).

Supplementary Materials and Methods

Strains

Disruption of *PHO4* yielding the mutants *rsc3-ts pho4* and *arp9-ts pho4* was by transformation with a linear DNA fragment of the *PHO4* locus with a *URA3* marker gene cassette inserted into the *PHO4* ORF.

Plasmids

Plasmid pUC19-*PHO8*-short was used to assay samples from the WCE fractionation (Figure 1C), and was prepared by inserting a 2.7 kb PCR fragment generated with primers 5'-GGCCTGCAGAGTTAGATAGGATCAG-3' and 5'-CCGGATCCTCTTTCTCAGTAAGAG-3' and pP8apin (Hertel et al, 2005) as template via PstI and BamHI into pUC19. Plasmids used for generating all markers and for *in vitro* reconstitutions in Figures 2-4 and Supplementary Figure 2 were constructed by inserting respective 3.5 kb PCR fragments amplified with genomic DNA from strain BY4741 as template into the multiple cloning site of pUC19. The following primers and restriction enzymes were used:

pUC19-*PHO8*-long: 5'- CCATGTGCATAGGATCCGGACGTTTGCCATAGTGTTG -3' and 5'-CAGTCAGACGCTGCAGGGGAGAGTTAGATAGGATCAGT -3' via BamHI and PstI;

pUC19-*RIM9*: 5'-CATGTCGATTGAGCTCGCATCTTCTGCAACGCCTTG-3' and 5'-CAGTCAGTAAGGATCCCAGTGGATAGATTTCCGGAG-3' via SacI and BamHI;

pUC19-*CHA1*: 5'-CCATGTGCATTGGTACCTCTCAAACTGATTCGACCAC-3' and 5'-CAGTCAGTAATCTAGACAAGGGCAAATTGATGCTTC-3' via KpnI and XbaI;

pUC19-*SNT1*: 5'-CAGTCAAGCGTCTAGAAATGAGCGCAGAGCTATCAC-3' and 5'-CTCTGTGCATTCTGCAGGAGTGTTTGCGGATTGGATC-3' via XbaI and PstI;

pUC19-*RIO1*: 5'-CAGTCGGATGGAGCTCACTTCTATTGGCTTAGGAGC-3' and 5'-CACTGTGCATTTCTAGAACGACGAAGACGAGGATTAG-3' via SacI and XbaI;

pUC19-*RNR3*: 5'-CACTGTGCATTTCTAGACATCCAACTGGTCAAGGGGT-3' and 5'-CGTTCGTCTGGTCGACTCTTCCTGTTACATGCGTCC-3' via XbaI and SalI.

pUC19-*PHO5*: 5'-CCATGTGCTACGAATTCTCCTGTCCTTGTATTCGTCC-3' and 5'-CAGTCAGACGAAGCTTACTACAGGGATTGAAACATCC-3' via EcoRI and HindIII.

pUC19-*ADH2*: 5'-CCATGTGCATTGGTACCCGCTGTTATGTTCAAGGTCC-3' and 5'-CAGTCAGACGCTGCAGATCCTCAATCCAAGGCGAAC-3' via KpnI/PstI. pUC19-*PHO84* was as described (Wippo et al, 2009). The sequence of each entire insert was confirmed by dideoxy sequencing (data not shown).

Yeast whole cell extract (WCE) fractionation

Ten 1 ml aliquots of WCE were supplemented each with 176,5 mg of ammonium sulphate, and rotated in a wheel at 4 °C until all ammonium sulphate was dissolved (corresponding to 30% saturation). After centrifugation for 30 min at 4 °C at 26000 rpm (max RCF of 41500) in a Beckmann TLA55 rotor the supernatants were transferred to fresh tubes and another 92,4 mg each of ammonium sulphate were added to achieve 45% saturation. After centrifugation as before, the supernatants ("SN fraction") were pooled in a fresh tube. The pellets from the first centrifugation step ("30% fraction") were resuspended in 5 ml of Basic Buffer (80 mM KCl, 20 mM Hepes-KOH pH 7.5, 10 % glycerol, 5 mM DTT, 0.1 mM phenylmethylsulfonyl fluoride and 1 mM sodium metabisulfite). The pellets from the second centrifugation step ("45% fraction") were resuspended in 5 ml Basic Buffer plus 1 M ammonium sulphate. The "30% fraction" and the "SN fraction" as well as 500 µl of the "45 % fraction" were exhaustively dialysed against Basic Buffer. A 5 ml HP Phenyl Sepharose FF low-sub column (GE Healthcare) was equilibrated with Basic Buffer plus 1 M ammonium sulphate and loaded with the remaining 4.5 ml of the "45% fraction". The flow-through was collected and the column was step-eluted with Basic Buffer containing 500 or 200 or no ammonium sulphate. All fractions were exhaustively dialysed against Basic Buffer. Three 1 ml Heparin HP columns (GE Healthcare) were connected in series, equilibrated with Basic Buffer, and loaded with the 500 mM ammonium sulphate fraction from the Phenyl Sepharose column. The flow-through was collected, and further fractions obtained by step-elution with Basic Buffer plus 200mM, 400mM and 1000mM KCl, respectively. All fractions except for the flow-through were dialysed exhaustively against Basic Buffer. A 1 ml DEAE FF (GE Healthcare) column was equilibrated with Basic Buffer and loaded with the 400 mM KCl fraction from the Heparin column and the flow-through collected. The column was eluted step-wise with Basic Buffer plus 150mM, 350mM and 500mM KCl, respectively. All fractions except for the flow-through were exhaustively dialysed against Basic Buffer.

Mass Spectrometry

Slices from SDS-PAGE gels were washed twice with water and twice with 40 mM ammoniumbicarbonate each for 30 min. After two-times treatment with 50% acetonitrile for 5 min, trypsin (enzyme/protein ratio 1:20-1:100) (Sequencing Grade Modified, Promega) was added and proteins were digested overnight in 40 mM ammoniumbicarbonate at 37 °C while shaking (600 rpm). For protein identification probes/peptides were purified (desalted) using C18 ZipTips® (Millipore) prior to nano-ESI-LC-MS/MS. Each sample was then separated on a C18 reversed phase column via a linear acetonitrile gradient (UltiMate 3000 system (Dionex) and column (75 µm i.d. x 15 cm, packed with C18 PepMap™, 3 µm, 100 Å (LC Packings)) before MS and MS/MS spectra were recorded on an Oribitrap mass spectrometer (Thermo Fisher Scientific). The resulting spectra where analyzed via the Mascot™ Software (Matrix Science) using the Swiss-Prot Protein Database.

Indirect end labeling and restriction enzyme accessibility analysis

Secondary cleavage for DNaseI indirect end labeling was with the following restriction enzymes: *PHO8*: BglII, *PHO5*: ApaI, *RIM9*: HpaI, *CHA1*: BamHI, *SNT1*: SspI, *RIO1*: HpaI (Figure S6) or BamHI (Figure S7E), *RNR3*: PstI, *GAL10*: HpaI, *ADH2*: HindIII and *PHO84*: SspI. For restriction enzyme accessibility assays at the *PHO8* promoter samples were digested with BglII and EcoRV. The probes for DNaseI indirect end labeling and restriction enzyme assays were generated by PCR using the following primers and either a pUC19 plasmid carrying the corresponding locus (were available) or genomic yeast DNA as template. *PHO8*: 5'-GACGGATCTCGAAGAGATCA-3' and 5'-CCTGCCATCTGTAATCAACA-3'; *PHO5*: 5'-GTCTTCAGCGTCAACTTTAG-3' and 5'-GCCAATGTGCAGTAGTAACT-3'; *PHO84*: 5'-CCTTGAGAACTTCAGTTGAC-3' and 5'-GAGTGAAGGCCATCAAAATC-3'; *RIM9*: 5'-GTGACCGAGTTAGCACAACC-3' and 5'-CATTGCTTCAACGCTCGAAG-3'; *CHA1*: 5'-CATGTCAAAGACTGTCTCTAC-3' and 5'-CCATACCTTTCCAAACCTTG-3'; *SNT1*: 5'-TGAAAAGAACAGGTCCGTCG-3' and 5'-CGAAATTAATCATGTCCCAG-3'; *RIO1* (Figure S6): 5'-CTAAACTCATTGGATGTTCA-3' and 5'-GTCTTAGATCCGAGAACTAT-3'; *RIO1* (Figure S7E): 5'-CTTCATACTGGCCTGTTTCC-3' and 5'-TTGTCTGTGTCGCAAGGTGC-3'; *RNR3*: 5'-TGCTCCTATGATTTCGGACG-3' and 5'-GATAGAGTCATCCTTCATGGC-3';

ADH2: 5'-AGAATACGCTACCGCTGACG-3' and 5'-ATTGATGATACCGTGGGCAC-3';
GAL10: 5'-TCTGCAACGACCGTAATACG-3' and 5'-GGAAGTTCGATTTGCCGTTG-3'.

Markers

Marker fragments were generated by digesting the pUC19 plasmids carrying the corresponding locus with the following combinations of restriction enzymes:
PHO8: SacI/BglII, HindIII/BglII, EcoRV/BglII; NdeI/BglII;
RIM9: NheI/HpaI, SphI/HpaI, BglII/DraI, XbaI/NsiI;
CHA1: NciI/BamHI, HindIII/BamHI, EcoRV/BamHI, HaeII/BamHI;
SNT1: KpnI/SspI, MspI/SspI, SacI/SspI, SpeI/SspI;
RIO1: FokI/BamHI, NciI/BamHI, DraI/BamHI, HhaI/BamHI;
RNR3: BanII/PstI, AvaII/PstI, ApaI/PstI, ClaI/PstI;
PHO5: DraI/ApaI, ClaI/ApaI, BamHI/ApaI, FokI/ApaI;
ADH2: EcoRV/HindIII, SphI/HindIII, DpnI/HindIII, SacI/HindIII;
PHO84: ClaI/SspI, AgeI/SspI, ApaI/SspI, BsrBI/SspI;
GAL10: AgeI/HpaI, AvaI/HpaI, EcoRI/HpaI.

Preparation of figures

Hybridized Southern blots were exposed to X-ray films (Fuji Super RX) at −80 °C using intensifier screens (DuPont, Lightening Plus). If individual lanes differed significantly in signal strength, blots were exposed for varying times. Films were scanned in grey-scale modus (MikroTek ScanMaker i900) and image files imported in Adobe Photoshop CS2. Scan images of lanes from films with different exposure times were combined within one figure in order to obtain more even signal strength across the figure. All plots and images were imported in CorelDraw X3 for final figure layout.

Supplementary References

Badis G, Chan ET, van Bakel H, Pena-Castillo L, Tillo D, Tsui K, Carlson CD, Gossett AJ, Hasinoff MJ, Warren CL, Gebbia M, Talukder S, Yang A, Mnaimneh S, Terterov D, Coburn D, Li Yeo A, Yeo ZX, Clarke ND, Lieb JD, Ansari AZ, Nislow C, Hughes TR (2008) A library of yeast transcription factor motifs reveals a widespread function for Rsc3 in targeting nucleosome exclusion at promoters. *Mol Cell* **32:** 878-887

Barbaric S, Fascher KD, Horz W (1992) Activation of the Weakly Regulated PHO8 Promoter in Saccharomyces-Cerevisiae - Chromatin Transition and Binding-Sites for the Positive Regulatory Protein Pho4. *Nucleic Acids Research* **20:** 1031-1038

Damelin M, Simon I, Moy TI, Wilson B, Komili S, Tempst P, Roth FP, Young RA, Cairns BR, Silver PA (2002) The genome-wide localization of Rsc9, a component of the RSC chromatin-remodeling complex, changes in response to stress. *Mol Cell* **9:** 563-573

Floer M, Wang X, Prabhu V, Berrozpe G, Narayan S, Spagna D, Alvarez D, Kendall J, Krasnitz A, Stepansky A, Hicks J, Bryant GO, Ptashne M (2010) A RSC/nucleosome complex determines chromatin architecture and facilitates activator binding. *Cell* **141:** 407-418

Ghaemmaghami S, Huh WK, Bower K, Howson RW, Belle A, Dephoure N, O'Shea EK, Weissman JS (2003) Global analysis of protein expression in yeast. *Nature* **425:** 737-741

Hartley PD, Madhani HD (2009) Mechanisms that Specify Promoter Nucleosome Location and Identity. *Cell* **137:** 445-458

Hertel CB, Langst G, Horz W, Korber P (2005) Nucleosome stability at the yeast PHO5 and PHO8 promoters correlates with differential cofactor requirements for chromatin opening. *Molecular and Cellular Biology* **25:** 10755-10767

Jiang C, Pugh BF (2009) A compiled and systematic reference map of nucleosome positions across the Saccharomyces cerevisiae genome. *Genome Biol* **10:** R109

Ng HH, Robert F, Young RA, Struhl K (2002) Genome-wide location and regulated recruitment of the RSC nucleosome-remodeling complex. *Genes Dev* **16:** 806-819

Parnell TJ, Huff JT, Cairns BR (2008) RSC regulates nucleosome positioning at Pol II genes and density at Pol III genes. *Embo Journal* **27:** 100-110

Szerlong H, Saha A, Cairns BR (2003) The nuclear actin-related proteins Arp7 and Arp9: a dimeric module that cooperates with architectural proteins for chromatin remodeling. *EMBO J* **22:** 3175-3187

Venters BJ, Pugh BF (2009) A canonical promoter organization of the transcription machinery and its regulators in the Saccharomyces genome. *Genome Res* **19:** 360-371

Wippo CJ, Krstulovic BS, Ertel F, Musladin S, Blaschke D, Sturzl S, Yuan GC, Horz W, Korber P, Barbaric S (2009) Differential Cofactor Requirements for Histone Eviction from Two Nucleosomes at the Yeast PHO84 Promoter Are Determined by Intrinsic Nucleosome Stability. *Molecular and Cellular Biology* **29:** 2960-2981